

# Adhesion of chromium metallization on alumina surfaces prepared by sol–gel techniques

H. KANAI\*, G. J. DEMOTT†, D. L. KOHLSTEDT‡

*Department of Materials Science and Engineering, Cornell University, Ithaca, NY 14853, USA*

The adhesion of a sputter-deposited Cr metallization layer to alumina films prepared by a solution–gelation method has been investigated using a pull test. Alumina films with a range of thicknesses (1 to 6  $\mu\text{m}$ ) were prepared by dipping commercially available polycrystalline alumina substrates into hydrolysed aluminium butoxide sols and fired for 1 h at 500, 900, or 1200 °C. Monolithic, crack-free films resulted both from pure alumina and Ti-doped alumina sols. The adhesion strength was dependent on the thickness of the alumina films, as well as on the temperature of the heat treatment. Failure occurred in part between the alumina film and the substrate and in part between the alumina film and the chromium layer. For alumina films fired at 500 °C, the adhesion strengths of 1  $\mu\text{m}$  thick films were greater than those measured for 3 and 6  $\mu\text{m}$  thick films because of the formation of greater mechanical bonds between alumina films and the substrate. The adhesion strength of the chromium layers was greatly improved by firing at 1200 °C. This increase in adhesion strength was attributed to an increase in the surface roughness of these specimens, which occurred due to crystallization of the sol layer. The adhesion strengths of films doped with Ti was not significantly different from those of the undoped films.

## 1. Introduction

The use of ceramic substrate materials for chip carriers and other integrated circuitry applications has greatly increased interest in the study of metal–ceramic bonding. Commonly, alumina substrates are employed to support conductor patterns of copper or gold that are deposited over an adhesive layer, such as chromium, which adheres strongly to the ceramic substrate as well as to the conductor layer [1]. Although Cr, Ti, Ni, W, Mo, and Pd all adhere well to alumina substrates and two- or three-metal systems are sometimes utilized in industrial production [2], chromium has been used most extensively.

A substantial amount of work has been done in the area of metal–ceramic adhesion [3–7]. Chopra [8] reported that adhesion of a metal film to a ceramic substrate is generally the result of a bond with an oxide layer: consequently, adhesion strength was closely related to the free energy of formation of the metal oxide. Caulton and co-workers [9] found that the addition of oxygen during the initial deposition of chromium improved the adhesion strength between chromium and glass by several orders of magnitude. Pierce and Vaughan [10], who investigated the effect of oxygen partial pressure on the adhesion of chromium thin films to alumina substrates, concluded that the incorporation of oxygen resulted in increased adhesion strength because  $\text{Cr}_2\text{O}_3$  formed at the interface.

Although the formation of a  $\text{Cr}_2\text{O}_3$  layer at the interface between Cr and  $\text{Al}_2\text{O}_3$  appears to be important for good adhesion, the effects of surface morphology and impurities on the adhesion strength of a Cr film to ceramic surfaces have not been clarified. This report details an experiment in which the surfaces of alumina substrates were modified with alumina thin films prepared by sol–gel techniques to change these two parameters in thin surface layers. The morphologies of the alumina thin films formed on the substrates and the adhesion of sputter-deposited Cr pads on the alumina thin films are described. Titanium was chosen as a dopant because a thin “adhesive” layer of Ti has been shown to increase the adhesion between conductor layers and ceramic substrates.

## 2. Experimental procedure

Alumina sols were prepared by the hydrolysis of aluminium sec-butoxide,  $\text{Al}(\text{OC}_4\text{H}_9)_3$ , which is abbreviated as  $\text{Al}(\text{O}i\text{Bu})_3$  [11, 12]. The alkoxide was first diluted to 10 wt % with sec-butanol, then this solution was slowly introduced into vigorously stirred, distilled water at 90 °C. The mole ratio of water to the alkoxide was 100. stirring was continued for 30 min after the addition. At this point, concentrated HCl was added dropwise to the sol until the mole ratio of HCl to the alkoxide was 0.07. The sol was stirred for 4 h after the addition of HCl.

\* Present address: Toshiba Corporation, Research and Development Center, 1 Komukai, Toshiba-cho, Saiwai-ku, Kawasaki, 210 Japan

† Present address: Corning Glass Works, Corning, NY14831, USA

‡ Present address: University of Minnesota, Department of Geology and Geophysics, Pillsbury Hall, Minneapolis, MN 55455, USA.

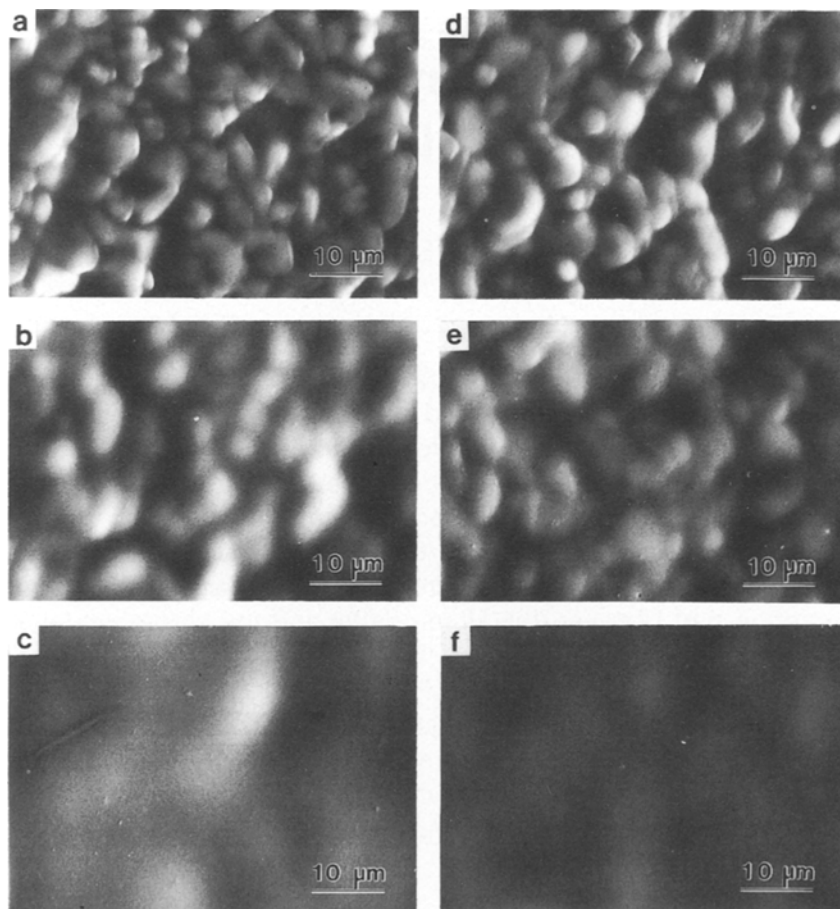


Figure 1 SEM micrographs of undoped films on polycrystalline  $\alpha$ -alumina substrate. (a) unfired, 1  $\mu\text{m}$ ; (b) unfired, 3  $\mu\text{m}$ ; (c) unfired, 6  $\mu\text{m}$ ; (d) 500  $^{\circ}\text{C}$ , 1  $\mu\text{m}$ ; (e) 500  $^{\circ}\text{C}$ , 3  $\mu\text{m}$ ; (f) 500  $^{\circ}\text{C}$ , 6  $\mu\text{m}$ ; (g) 900  $^{\circ}\text{C}$ , 1  $\mu\text{m}$ ; (h) 900  $^{\circ}\text{C}$ , 3  $\mu\text{m}$ ; (i) 900  $^{\circ}\text{C}$ , 6  $\mu\text{m}$ ; (j) 1200  $^{\circ}\text{C}$ , 1  $\mu\text{m}$ , (k) 1200  $^{\circ}\text{C}$ , 3  $\mu\text{m}$ , (l) 1200  $^{\circ}\text{C}$ , 6  $\mu\text{m}$ .

To prepare the doped sol, a 4 wt% solution of  $\text{Ti}[\text{O}(\text{CH}_2)_3\text{CH}_3]_4$  in sec-butanol was added to the solution of  $\text{Al}(\text{OBU})_3$  so that the mole ratio of dopant to aluminum was 0.05. This mixture was stirred for 10 min before it was slowly added to the stirred, 90  $^{\circ}\text{C}$  distilled water. The remaining sol preparation was the same as for the undoped sol.

Alumina films were prepared by dipping polycrystalline  $\alpha$ -alumina substrates into the sols. Film thickness was changed by single dipping the substrates into sols of increasing viscosity or by double dipping. The coated specimens were dried at 60  $^{\circ}\text{C}$  for 5 days and then fired at 500, 900, or 1200  $^{\circ}\text{C}$  for 1 h in air. The heating rate was 100  $^{\circ}\text{C h}^{-1}$ , and the cooling rate was 400  $^{\circ}\text{C h}^{-1}$ . Film thickness was measured on scanning electron microscope (SEM) micrographs of fractured cross-section.

A portion of each sol was poured into a glass petri dish, dried, and fired at the same schedule and temperatures as the thin film specimens. The phases formed were identified by the powder X-ray diffraction (XRD) method using a Cu target.

Twelve Cr pads (3 mm in diameter and 800 nm thick) were sputter-deposited on to each thin film specimen. A 0.63 mm diameter Mo wire was epoxied to each Cr pad. Failure force was measured by pulling the wire along a direction perpendicular to the substrate, using a screw-driven testing machine (Instron Model 1125 Tensile Strength Testing Machine), until separation. The crosshead speed of the testing ma-

chine was 2.5 mm  $\text{min}^{-1}$ . The failure stress was calculated by dividing the failure force by the pad area. The average value and standard deviation were calculated from the results of twelve such measurements.

Compositional analysis was performed with an electron microprobe (JEOL Superprobe 733) operating at the following conditions: 8 kV accelerating voltage, 17 nA reference current, 1  $\mu\text{m}$  beam diameter, and 20 s count time. Pure metal standards were used.

### 3. Results

#### 3.1 Morphology

SEM micrographs of both the unfired and the fired undoped films are shown in Fig. 1. These micrographs illustrate that the 1  $\mu\text{m}$  thick films conform to the surface of the substrates and that the roughness of the films decreases as the thickness increases. In general, the surfaces of the films were quite smooth for the specimens fired below 900  $^{\circ}\text{C}$ . The formation of 0.1 to 0.2  $\mu\text{m}$  thick lamellae during the 1200  $^{\circ}\text{C}$  firing is also illustrated in this figure.

The general trends in surface morphology of the Ti-doped specimens were similar to those of the undoped specimens.

#### 3.2 Phase determination

The XRD patterns of the undoped gels gave the following results: the diffuse diffraction pattern of the

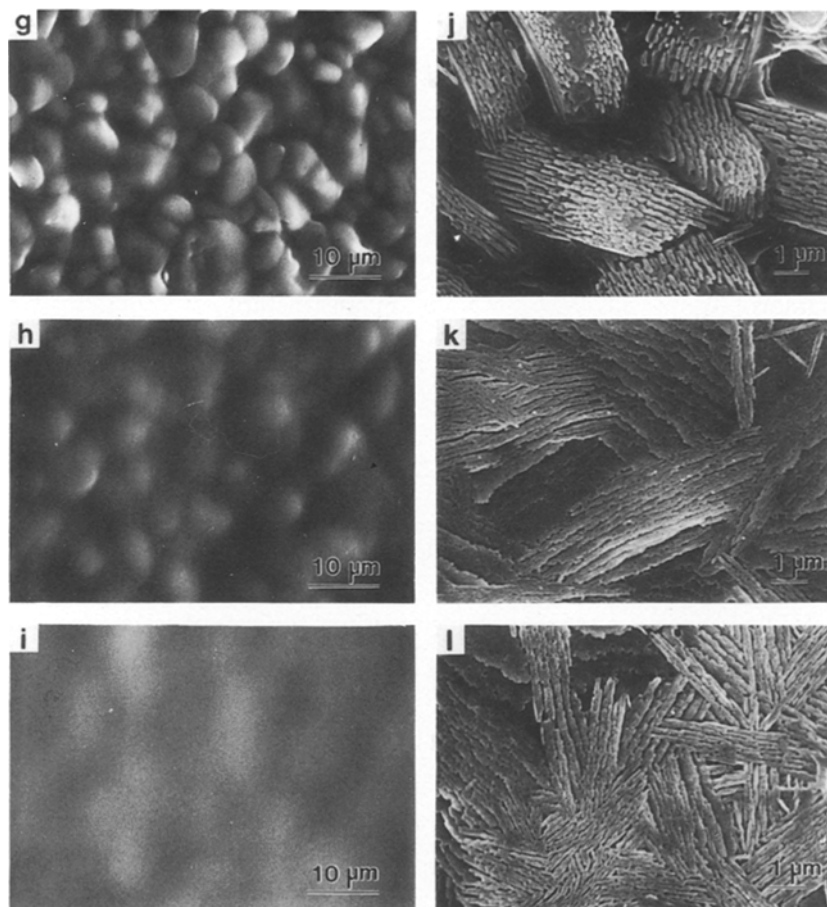


Figure 1 Continued

unfired gel corresponds to that of boehmite. Although the XRD pattern of the gel fired at 500 °C showed the presence of  $\gamma\text{-Al}_2\text{O}_3$  and the pattern of the gel fired at 900 °C showed the presence of  $\delta\text{-Al}_2\text{O}_3$ , these patterns were quite broad, indicating incomplete crystallization. In contrast, the XRD peaks of the specimens fired at 1200 °C were sharp and indicated the presence of completely crystallized  $\alpha\text{-Al}_2\text{O}_3$ .

The XRD patterns for doped specimens which were fired at 500 and 900 °C were featureless, indicating amorphous structures. The XRD patterns of the Ti-doped specimens that were fired at 1200 °C revealed the presence of  $\alpha\text{-Al}_2\text{O}_3$  plus  $\text{TiO}_2$ .

### 3.3 Compositional analysis

Electron microprobe analysis of the Ti-doped specimens fired at 500 and 900 °C indicates that these specimens are compositionally homogeneous, with  $6.4 \pm 0.6$  wt %  $\text{TiO}_2$ . The Ti-doped specimen fired at 1200 °C separated into regions of pure alumina and regions of  $\text{TiO}_2$  plus  $\text{Al}_2\text{O}_3$ , as predicted by the phase diagram for the  $\text{Al}_2\text{O}_3\text{-TiO}_2$  system.

### 3.4 Failure stress measurements

The results of the pull tests are shown in Table I. These results reveal several trends: (1) For specimens fired at 500 °C, the failure stress was greater for the 1  $\mu\text{m}$  thick film than for the 3 and 6  $\mu\text{m}$  thick films. (2) The failure

stresses for the specimens fired at 500 °C are slightly greater than those for the specimens fired at 900 °C. (3) The failure stress is the highest for specimens fired at 1200 °C; at this temperature all of the pull tests failed in the epoxy. (4) The failure stresses for the Ti-doped specimens were similar to those measured for the undoped specimens of the same thickness. The pull test also failed in the epoxy during failure stress measurements performed on twelve Cr pads that were deposited on an uncoated alumina substrate specimen.

TABLE I Pull test failure stress measurements

Dopant	Film thickness ( $\mu\text{m}$ )	Failure stress (MPa)		
		500 °C	900 °C	1200 °C
None	1	$1.3 \pm 0.3$	$0.7 \pm 0.2$	$\sigma > \sigma_{\text{ep}}$
	3	$0.4 \pm 0.2$	$0.2 \pm 0.0$	$\sigma > \sigma_{\text{ep}}$
	6	$0.8 \pm 0.3$	$0.6 \pm 0.1$	$\sigma > \sigma_{\text{ep}}$
Ti	1	$1.5 \pm 0.3$	$1.0 \pm 0.5$	$\sigma > \sigma_{\text{ep}}$
	3	$0.7 \pm 0.2$	$0.3 \pm 0.2$	$\sigma > \sigma_{\text{ep}}$
	6	$0.9 \pm 0.3$	$0.7 \pm 0.4$	$\sigma > \sigma_{\text{ep}}$

Note:  $\sigma > \sigma_{\text{ep}}$  denotes that the adhesion is greater than the strength of epoxy.

## 4. Discussion

As firing temperature is increased, an alumina gel undergoes the following phase transformation [13]: boehmite- $\gamma$ -alumina- $\delta$ -alumina- $\alpha$ -alumina. Although these phases were observed in this study, the specimens which were fired at 500 and 900 °C exhibited incomplete crystallization due to the short firing times. The phases formed in both the undoped and the Ti-doped specimens fired at 1200 °C conformed to published phase diagrams [14].

According to Yoldas, alumina bulk materials prepared from aluminum sols are porous (porosity of 65%) with small pores having radii less than 5 nm and large pores having radii of 10 to 15 nm. Before the  $\alpha$ -Al<sub>2</sub>O<sub>3</sub> crystallization temperature of 1200 °C is reached, this porosity is essentially all eliminated, strengthening the material [15]. In our experiment, the relative density of undoped monolithic gel fired at 1200 °C for 1 h was 98%.

### 4.1 Undoped coatings

To determine the difference in strength of adhesion of 1  $\mu$ m thick films and 6  $\mu$ m thick films to the substrate, cross-sections of the samples fired at 500 °C were examined. It is difficult to distinguish the 1  $\mu$ m thick film from the substrate, Fig. 2a. The 6  $\mu$ m thick film is, however, easily distinguished from the substrate, Fig.

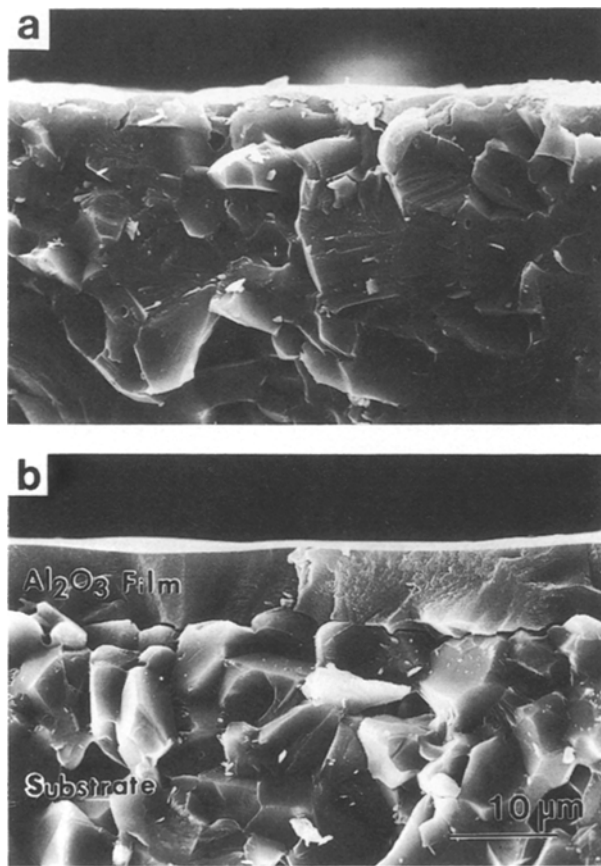


Figure 2 SEM micrographs of cross-sections of samples with (a) 1  $\mu$ m thick film and (b) 6  $\mu$ m thick film on polycrystalline  $\alpha$ -alumina substrates.

2b, because there are openings between the film and the substrate; that is, the 6  $\mu$ m thick film did not conform as well to the substrate surface. This situation was also observed with 3  $\mu$ m thick films. These results suggest that the bonding between 1  $\mu$ m thick film and the substrate should be greater than the bonding between the thicker films and the substrate. Consequently, the higher failure stresses observed for the 1  $\mu$ m thick films can be correlated directly with the microstructure.

The surfaces that were left behind after the pull test (failure areas) were examined by SEM. Micrographs of these failure areas from the undoped specimens which were fired at 500 and 900 °C are shown in Fig. 3. In some cases, fragments of the gel layer were removed with the Cr film during the pull test. Energy dispersive spectrometric (EDS) analysis of the gel layer fragments which remained attached to the substrate indicated that no Cr was left behind in any of these cases. The ratio of the area of gel coating which was removed by the pull test to the total area of the Cr pad – the “broken-area ratio” – was calculated from SEM micrographs of three different areas for each specimen shown in Fig. 3.

For the specimens fired at 500 °C the broken area ratios were  $0.05 \pm 0.01$  for 1  $\mu$ m thick films,  $0.26 \pm 0.03$  for 3  $\mu$ m thick films, and  $0.14 \pm 0.04$  for 6  $\mu$ m thick films, thus, failure occurred primarily by debonding at the interface between the metal and the ceramic thin films.

For the specimens which were fired at 900 °C, the broken area ratios were  $0.20 \pm 0.07$  for 1  $\mu$ m thick films, and  $1.00 \pm 0.00$  for both the 3 and the 6  $\mu$ m thick films. In this case, failure occurred by debonding at the gel film–substrate interface. To investigate the cause of the lower adhesion strength of the specimens which were fired at 900 °C, the expansion of the undoped films during firing was measured. The spacings between indentations in the coating did not change for specimens that were fired at 500 °C, however, the spacings increased by 5% for specimens that were fired at 900 °C. This change indicates that the coating is expanding at this firing temperature. This expansion may be caused by the evolution of structural water and residual organics during firing at this temperature [16], which quite likely causes microfracturing of the gel film–substrate interface.

For undoped samples fired at 1200 °C, transmission electron micrographs (TEM) of cross-sections of these specimens reveal a porous structure made up of approximately 100 nm diameter particles joined by sintered necks, as shown in Fig. 4. This structure is similar to the vermicular  $\alpha$ -alumina particles observed by Dynys and Holloran [17]. TEM micrographs of the gel–substrate interface region of these undoped specimens demonstrate that the gel film is sintered to the substrate in several places, as illustrated in Fig. 5. The direct sinter-bonding of the gel film to the substrate, combined with the open, lamellar structure of the films into which Cr metal could be deposited, results in the high adhesion strengths measured for the metal–gel film–substrate systems formed under these conditions.

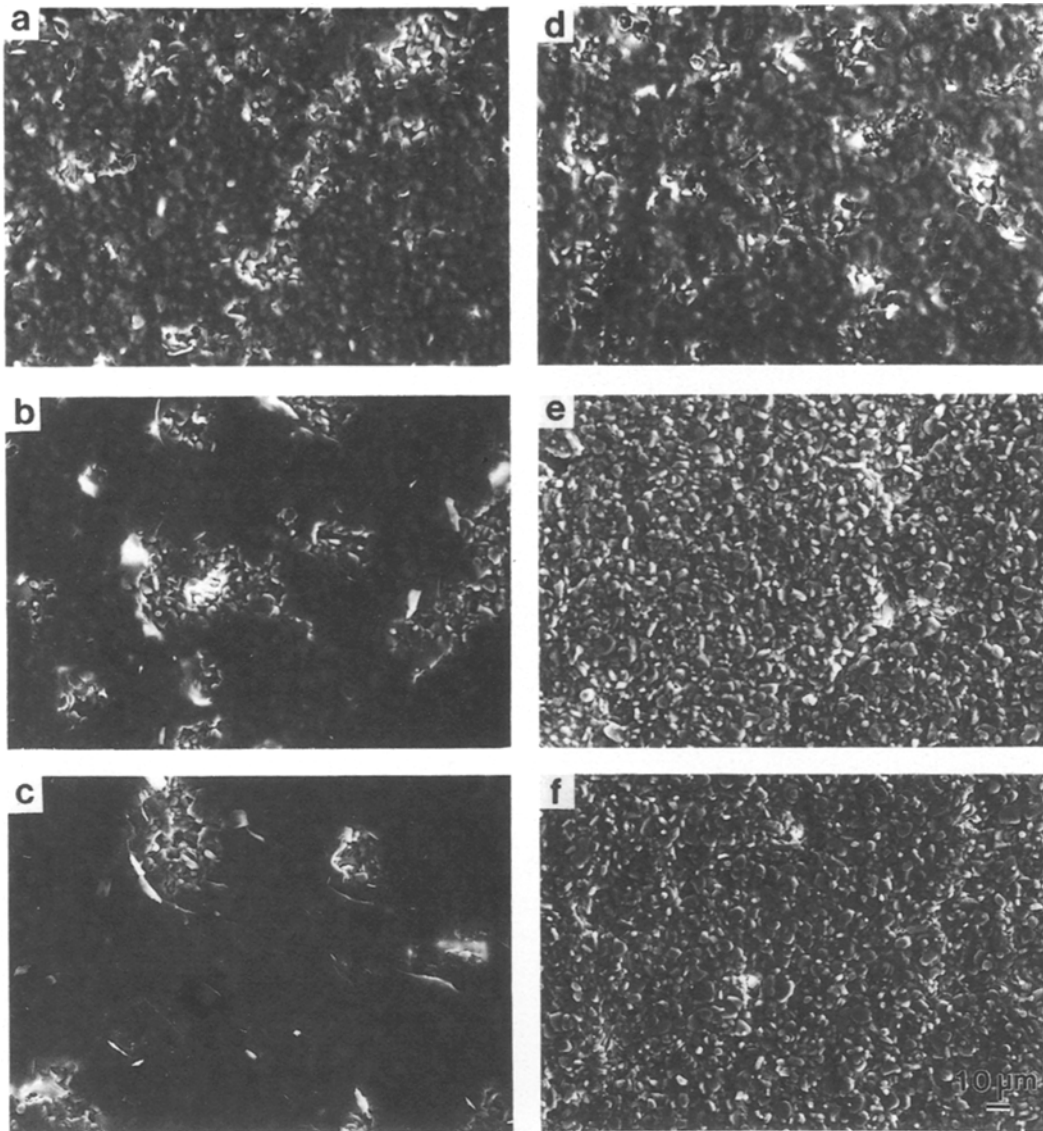


Figure 3 SEM micrographs of failure areas on undoped films that had been fired at 500 or 900 °C for 1 h (a) 500 °C, 1 μm; (b) 500 °C, 3 μm; (c) 500 °C, 6 μm; (d) 900 °C, 1 μm; (e) 900 °C, 3 μm, (f) 900 °C, 6 μm.

#### 4.2 Ti-doped coatings

The surface roughness of the specimens which were doped with Ti is very similar to that of the undoped homologues. In addition, the broken area ratios of the

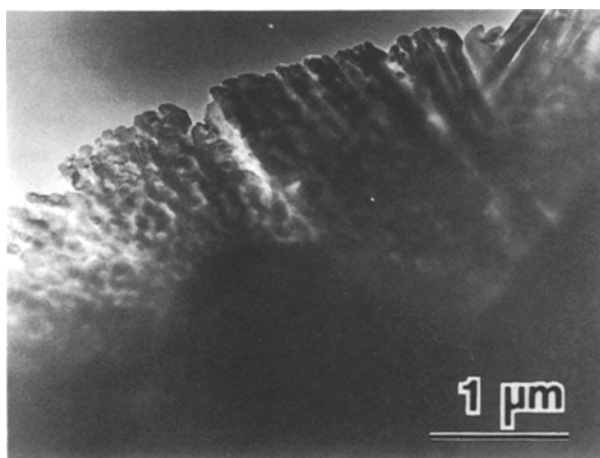


Figure 4 TEM micrograph of cross-section of undoped gel film fired at 1200 °C, revealing a vermicular structure.

Ti-doped specimens could not be distinguished from those of the undoped specimens. Within the scatter in the data, the failure stresses determined for the Ti-doped films were also identical to those measured for undoped films. Therefore, the addition of Ti, at these concentrations, to alumina films does not affect either the adhesion of sputter-deposited Cr films to the gel films or the adhesion of the gel films to the alumina substrates. This result suggests that, in the present study with relatively rough  $\text{Al}_2\text{O}_3$  surfaces, mechanical bonding between chromium and alumina dominates metal-ceramic adhesion.

#### 5. Summary and conclusions

Monolithic, crack-free thin (1 to 6 μm thick) films of pure  $\text{Al}_2\text{O}_3$  were formed by dip coating polycrystalline alumina substrates with an average grain size of 10 μm into sols that were formed by hydrolysis of  $\text{Al}(\text{O}i\text{Bu})_3$ . Thin alumina films doped with Ti were also prepared. The adhesion failure stress of Cr films that were sputter-deposited on the gel films after they were fired was determined by a pull test method. The

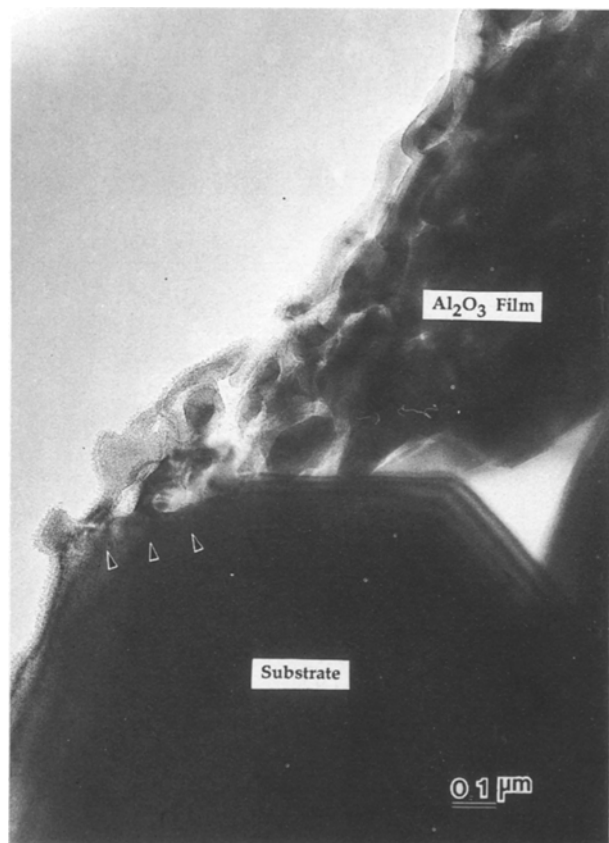


Figure 5 TEM micrograph of cross-section of undoped gel film fired at 1200°C, revealing a well sintered interface between the gel film and the substrate.

failure stress was dependent on the thickness of the gel film and on the heat treatment, with the highest failure stresses determined for the specimens with the roughest gel-coated surface (i.e., for all specimens which were fired at 1200°C). No direct effect of the composition of the gel dopant could be determined.

## Acknowledgments

This work was supported by IBM through the Cornell Ceramics Program. The electron microscopy and X-ray diffraction were carried out in central facilities of the National Science Foundation Materials Science Center at Cornell University. GJD was supported by Corning Glass Works, and HK was supported by Toshiba Corporation.

## References

1. L. G. BHATGADDE and S. MAHAPATRA, *Met. Finishing* (1987) 55-57.
2. P. H. HOLLOWAY, *Gold Bulletin* **12** (1979) 99.
3. J. STRONG, *Rev. Sci. Instrum.* **6** (1935) 97.
4. L. HOLLAND, in "Vacuum deposition of thin films" (Wiley, New York, 1956) p. 102.
5. P. BENJAMIN and C. WEAVER, *Proc. R. Soc.* **A254** (1960) 163.
6. P. BENJAMIN and C. WEAVER, *ibid.* **A274** (1963) 267.
7. M. M. KARNOWSKI and W. B. ESTILL, *Rev. Sci. Instrum.* **35** (1964) 1324.
8. K. L. CHOPRA, in "Thin film phenomena" (McGraw-Hill, New York, 1969) p. 321.
9. M. CAULTON, W. L. SKED and F. S. WOZNIAK, *RCA Rev.* **40** (1979) 115.
10. R. W. PIERCE and J. G. VAUGHAN, *IEEE Trans. on Comp., Hybrids, and Manuf. Tech.* **6** (1983) 202.
11. B. E. YOLDAS, *Amer. Ceram. Soc. Bull.* **54** (1975) 289.
12. A. C. PIERRE and D. R. UHLMANN, *J. Amer. Ceram. Soc.* **70** (1987) 28.
13. R. K. DWIVEDI and G. GOWDA, *J. Mater. Sci. Lett.* **4** (1985) 331.
14. E. M. LEVIN, C. R. ROBBINS and H. F. MCMURDIE, (eds) in "Phase diagrams for ceramists" (The American Ceramic Society, Columbus, OH, 1964) p. 123.
15. B. E. YOLDAS, *Amer. Ceram. Soc. Bull.* **54** (1975) 286.
16. D. E. CLARK and J. J. LANNUTTI, in "Ultrastructure Processing of Ceramics, Glass, and Composites" (John Wiley, New York, 1984) pp. 126-141.
17. F. W. DYNYS and J. W. HOLLORAN, in "Ultrastructure Processing of Ceramics, Glass, and Composites" (John Wiley, New York, 1984) pp. 142-151.

Received 29 May  
and accepted 26 June 1990